

# **Collaboration with NUS MD6 iHealthTech in developing anti-IL11 antibody (X203) Layer-by-Layer (LbL) Nanoparticles to achieve Prolonged Sustained Released Effects for Therapeutic Applications**

**Riffaie Fathan B Rahim & Nuruddini Hidni Binte Khalid**

**Supervisor: Dr Yang Fei Tan (NUS) & Dr Raja RANGASWAMY (TP)**

## **Abstract**

*This project aims to design and fabricate anti-IL-11 antibody (X203) layer-by-layer nanoparticles to achieve prolonged sustained released effects for therapeutic applications. Anti-IL-11 antibodies (X203) were incorporated into the layer-by-layer nanoparticles (NP) system utilized as nanocarriers. Fabricated single-layered X203 LbL NPs had characterization values of  $441.80 \pm 20.90$  in hydrodynamic size, a polydispersity index (PDI) of  $0.30 \pm 0.16$ , and a surface charge of  $27.00 \pm 1.15\text{mV}$ . While fabricated double-layered X203 LbL NPs had characterization values of  $439.17 \pm 8.49$  in hydrodynamic size, a polydispersity index (PDI) of  $0.39 \pm 0.15$ , and a surface charge of  $10.45 \pm 2.68\text{mV}$ . The successfully fabricated X203 LbL NPs were then used to conduct release studies to determine their release activity, providing a controlled release effect of up to 14 days for single-layered X203 LbL NPs, and up to 70 days for the double-layered X203 LbL NPs. Thus, the fabricated LbL nanoparticle systems meet the project's objective of achieving a prolonged sustained release effect.*

## **1. INTRODUCTION**

### **1.1 Background**

Interleukin-11 (IL-11), a multifunctional hematopoietic cytokine belongs to the interleukin-6 (IL-6) family of cytokines utilizing the GP-130 signaling pathway shared by other cytokines of the same family [1]. They are secreted by osteoblasts, synoviocytes, fibroblasts,

chondrocytes, intestinal myofibroblasts, and trophoblasts. IL-11 are considered primarily anti-inflammatory and found in the plasma during inflammation.

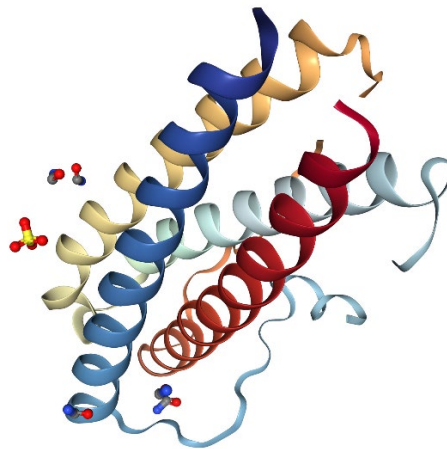


*Figure 1. 1 Interleukin 11 protein structure*

IL-11 helps stimulate hematopoiesis and thrombopoiesis, regulates macrophage differentiation, and confers mucosal protection in the intestine. In addition, has been found to enhance T cell polarization towards Th2, promote the production of B cell IgG, increase absorption of osteoclast bone, protect endothelial cells from oxidative stress, and regulate epithelial proliferation and apoptosis [2]. However, IL-11 upregulation in the human lung has been linked with viral infections and several fibroinflammatory diseases, including idiopathic pulmonary fibrosis.

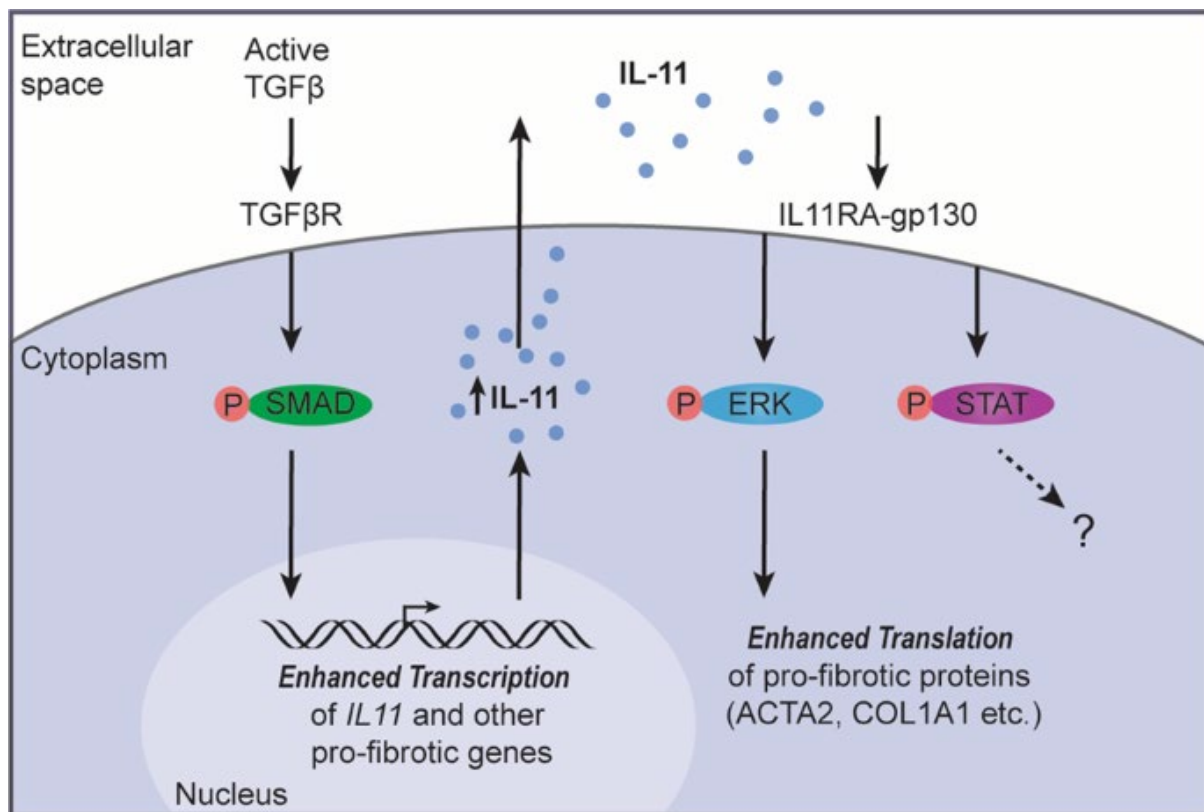


Figure 1. 2 Autocrine IL-11 signalling underlies fibroblast activation

Translation of profibrotic proteins can be triggered when transforming growth factor-beta (TGFβ) and other disease factors initiates an autocrine loop of IL-11 signaling in pulmonary fibroblasts in a largely ERK-dependent manner. Thus, IL-11 is now recognized as an important determinant of lung fibrosis, inflammation, and epithelial dysfunction. Anti-IL-11, an antibody that targets IL-11, has been known to arrest or even reverse bleomycin-induced pulmonary fibrosis and inflammation. [3]. Therefore, the downregulation of IL-11 might potentially be a therapeutic approach for the treatment of mentioned infections and diseases. Chronic diseases require a constant, sufficient, and prolonged duration of drug bioavailability; hence a prolonged and sustained release is required. A method of providing these therapeutic approaches is through the treatment of medication using nanocarriers. Nanocarriers are colloidal drug delivery systems that are submicron size of typically less than 500nm, providing efficient cellular entry, protection, loading, and slow release of active agents [4]. However, as nanocarriers are relatively new, most nanocarriers developed are unable to provide a slow and

controlled release of their active agents. As a result, is not patient-friendly and can lead to undesirable systemic side effects due to frequent administration for prolonged therapeutic effect [5]. Hence, to ensure the safe administration of active agents, nanocarriers developed should enable a controlled and sustained release of active agents for prolonged therapeutic effects. This in turn can improve patient adherence to treatments due to less frequent dosages.

## **1.2 Objectives**

The project aims to design and fabricate anti-IL-11 antibody (X203) layer-by-layer (LbL) nanoparticles to achieve prolonged sustained release effects for therapeutic applications.

The specific objectives of the project were to:

- Fabricate layer-by-layer nanoparticles incorporating anti-IL-11 antibody (X203) with specifications of:
  - Final LbL NP hydrodynamic configuration size of less than 500 nm.
  - Ensure successful coating of layers and encapsulation of antibody X203 in the LbL NPs.
- Characterize fabricated LbL NPs by acquiring following parameters:
  - Hydrodynamic size, surface charge, and polydispersity index (PDI).
  - Encapsulation efficiency (EE).
- Demonstrating prolonged sustained release effect of the fabricated and characterized nanocarriers through release studies.

## **2. PROJECT DESCRIPTION**

### **2.1 Physical description of the layer-by-layer nanoparticles**

LbL NPs are modular drug delivery systems that can incorporate considerable functional materials through the sequential deposition of polyelectrolytes onto charged nanoparticle cores [6]. They are effective transport agents due to their relatively small size and ability to modify their charge and shape to transport active therapeutic agents to tissues. The advantages of using these nanocarriers (LbL NPs) are their protection against degradation, sustained release, high loading, and cellular uptake [7].

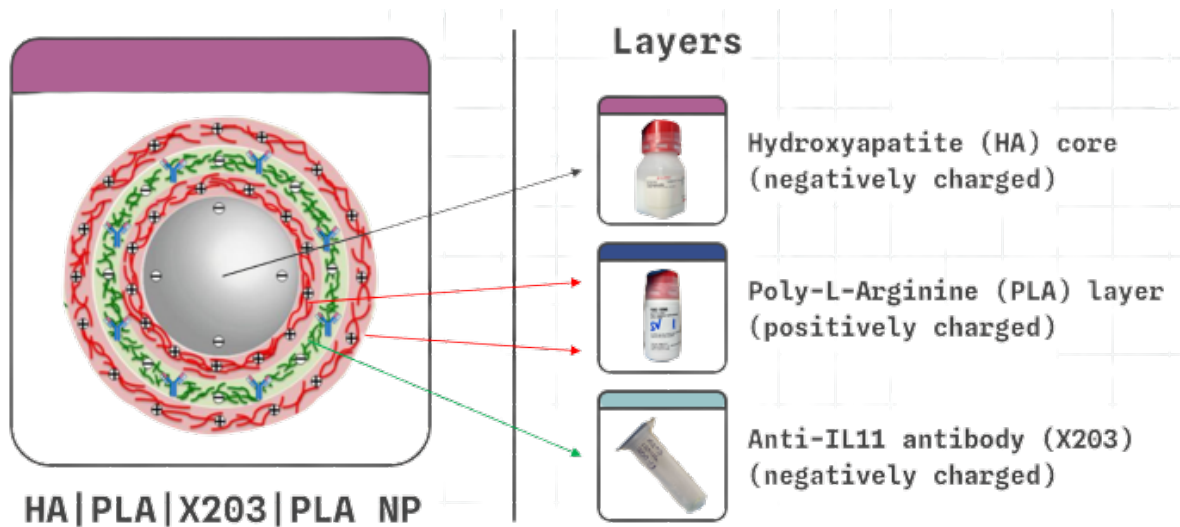


*Figure 2. 1 Single-layer HA X203 LbL NP Configuration*

Layers are coated through electrostatic interactions to form HA|X203 LbL NPs, where hydroxyapatite (HA) is used as a negatively charged structural core due to the presence of hydroxide ions [8]. HA core is coated with poly-l-arginine (PLA) which is positively charged due to the presence of a guanidino group [9]. Subsequently, X203 which was prepared in NaCl (0.1M, pH 9.5) giving it a negative charge is placed followed by the final layer of positively charged PLA [10].

## 2.2 Process description of the layer-by-layer nanoparticles

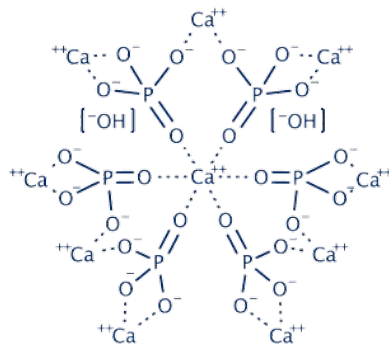


*Figure 2. 2 Hydroxyapatite (HA) structure*

Hydroxyapatite (HA) is used as the core structure as it is negatively charged due to the presence of hydroxide ions. HA particles were used for the LbL NPs as it is the most stable calcium phosphate derivative which makes it a good carrier for the release of substance as it does not disintegrate prematurely. Moreover, due to its mesoporous property, it can offer high active agent loading capacity and a sustained release through its reliable dissolution. In addition, HA is biodegradable and extremely biocompatible due to its chemical compatibility with biological mineralized bone which also makes them safe to use in the body. Hence, HA is used for the LbL NP core structure [8].

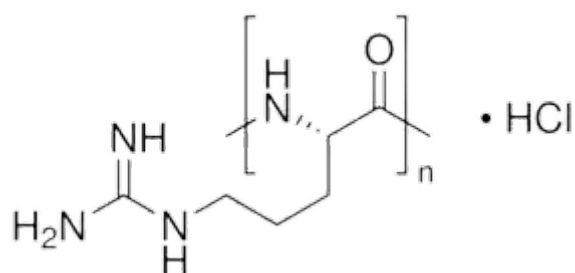


*Figure 2. 3 Poly-L-arginine structure*

Poly-L-arginine (PLA), a homopolyamino acid, is used as a layer due to its unique properties such as its high transfection efficiency and cellular uptake. In addition, it is biocompatible, representing a cationic biopolymer composition of physiologically active L-arginine amino acid. The presence of the guanidinium group is responsible for the net positive charge and hydrophobic character [9].

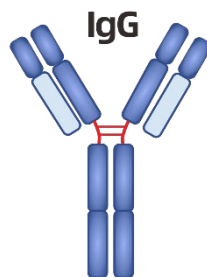


*Figure 2. 4 Antibody (X203) Structure*

Antibody X203 must be negatively charged to ensure solubility and successful coating between the positively charged PLA layers. Hence, it is prepared in NaCl (0.1M, pH 9.5), causing it to have a net negative charge. This is due to an antibody's isoelectric point (pI) of 8 – 9, where an antibody will carry a net negative charge when the pH is above the pI [10].

Furthermore, having coated the last layer with PLA helps protect the X203 from intracellular degradation, providing a prolonged and sustained release of the X203 as the PLA gradually defoliates.

### **3. PROJECT DEVELOPMENT**

#### **3.1 Research and development**

Necessary biochemical laboratory skills and knowledge were picked up before the commencement of the project. In addition, research was conducted regarding the technical aspects of the materials, preparation, and characterization methods of layer-by-layer nanoparticles. Moreover, techniques to determine drug release rates were also researched.

#### **3.2 Fabrication of HA|X203 LbL NPs**

Firstly, 2.5mg of HA were measured out to be dissolved in 1ml of pH 5.5 sodium chloride. The HA was then centrifuged at 4°C at a speed of 12000G for 10 minutes. The procedure was

performed twice to wash the HA nanoparticles. After the final wash, HA was resuspended in 250ul of NaCl (0.1M, pH 5.5). Secondly, 1.25mg of PLA were measured out to be dissolved in 2.5ml of NaCl (0.1M, pH 5.5) at a ratio of 0.5mg/ml. The HA will be added to the PLA in a volumetric ratio of 1:10 (HA:PLA), washed twice, and resuspended into 300ul of NaCl (0.1M, pH 5.5). Afterwards, 0.15mg of X203 dissolved in 1.5ml of NaCl (0.1M, pH 9.5) and 300ul of HA|PLA were loaded into two separate syringes and into an IGNITE machine, at a flow rate of 0.8ml/min and a flow rate ratio of 1:5 to formulate the HA|PLA|X203 with a total volume of 1.8ml. Lastly, 6mg of PLA was measured out to be dissolved in 1ml of NaCl (0.1M, pH 5.5), which will be used to coat the last layer to form HA|PLA|X203|PLA. Both PLA and HA|PLA|X203 will be loaded into separate syringes and into an IGNITE machine, set at a flow rate ratio of 1:1.5 with its flow rate unchanged at 0.8ml/min, with a total volume of 1ml. The HA|PLA|X203|PLA solution is then washed and centrifuged one last time to achieve the final LbL NP configuration. For the double-layer X203 NPs, the fabrication continues, with the process for the second layer of X203 and the final PLA layer being the same as the previous methodology.

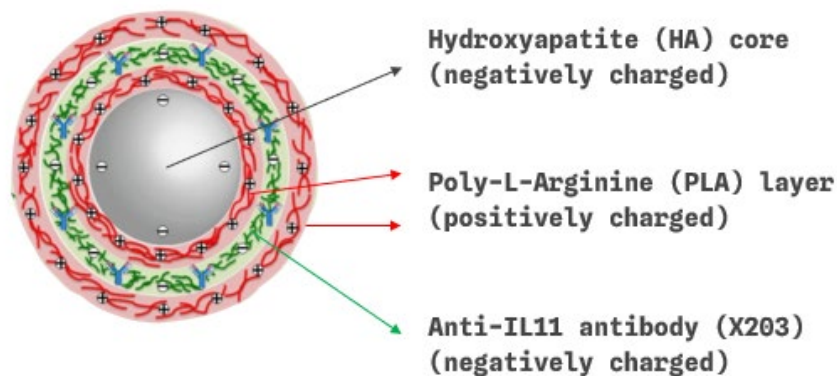


*Figure 3. 1 Single-layer HA X203 LbL NP Configuration*

### 3.3 Characterization of HA|PLA|X203|PLA LbL NPs





*Figure 3. 2 Malvern Zetasizer Nano ZS*

After successful coating of each layer, 10ul of sample is collected to be diluted in 900ul of deionized (DI) water to measure its hydrodynamic size and surface charge through dynamic light scattering (DLS) using its respective cuvette with a zetasizer (Malvern Zetasizer Nano ZS).

Serial dilution is performed using different concentrations of fluorescent-tagged X203 into 7 microtubes, which will then be scanned and measured inside a TECAN INF machine. A standard curve is drawn to determine its coefficient value and an  $R^2$  value of preferably  $\sim 0.99$ .

To determine its encapsulation efficiency (EE), the supernatant of the HA|X203 NP after washing is measured in the TECAN INF machine. Subsequently, the difference will be calculated between the amount loaded and the average of the supernatant to find the EE.

### **3.4 Conducting release studies of HA|PLA|X203|PLA LbL NPs**

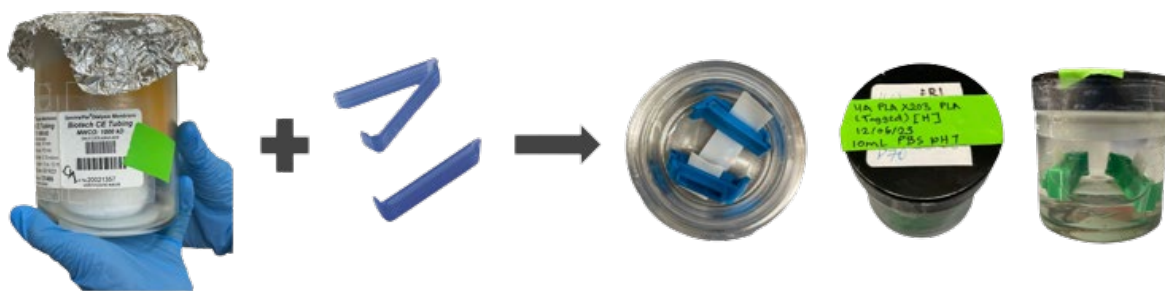


*Figure 3. 3 Procedure for bagging of HA X203 LbL NPs*

To conduct the release studies, 1ml of the fabricated and characterized HA|X203 LbL NPs were stored in dialysis tubings of size 1000kD, with the ends clamped with dialysis clips before being placed in a glass container containing 10ml of Phosphate Buffered Saline (PBS) as it mimics the human physiological condition at pH 7.4. It is then incubated inside an orbital shaker incubator at 37°C to simulate human body temperature. At each given time point, the release buffer is to be extracted inside the glass container and refreshed with fresh PBS, to be returned to the orbital shaker incubator.

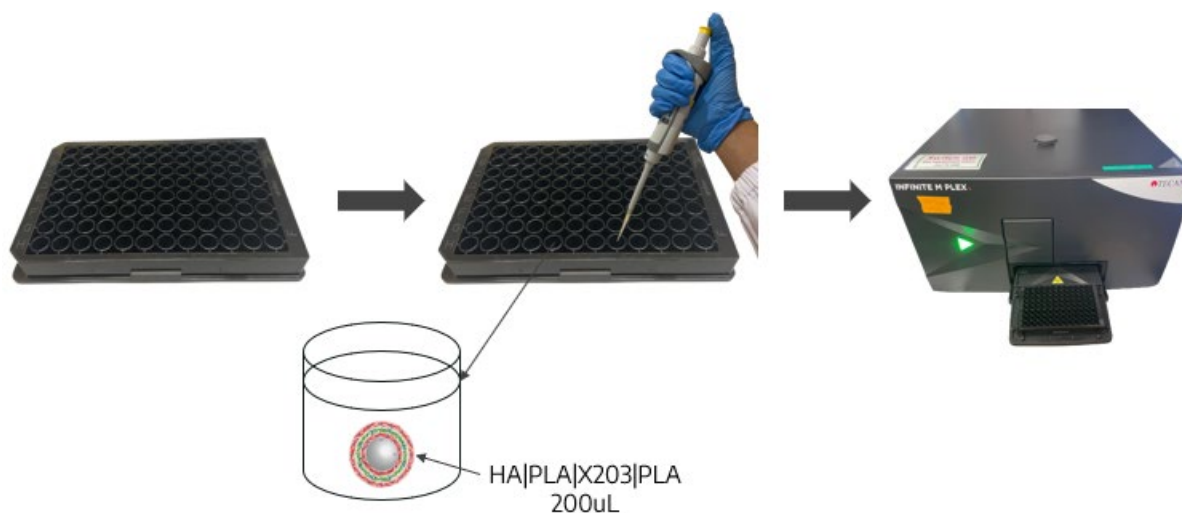


*Figure 3. 4 Procedure for conducting release studies of HA X203 LbL NPs*

The release buffer extracted is placed in a 96-well black plate. The release buffer is compared with a blank PBS to quantify the exact amount of X203 released. Once the release buffer and PBS have been placed in the 96-well black plate, it is measured in the TECAN INF machine

to find the amount of X203 release at the specific time point. The procedure was repeated until the total amount of X203 loaded in the LbL NPs is exhausted.

### 3.5 Statistical analysis

The experiments and measurements were conducted in triplicates (n = 3), in which the results are expressed as mean  $\pm$  standard deviation.

## 4. RESULTS AND DISCUSSIONS

### 4.1 Fabrication and characterization of HA|PLA|X203|PLA LbL NPs

Particle configurations	Zeta size (nm)	PDI	Zeta potential (mV)
HA  PLA	174.70 $\pm$ 3.84	0.24 $\pm$ 0.01	31.83 $\pm$ 2.20
HA  PLA  X203	363.77 $\pm$ 23.02	0.29 $\pm$ 0.01	-13.37 $\pm$ 1.21
HA  PLA  X203  PLA	441.80 $\pm$ 20.90	0.30 $\pm$ 0.16	27.00 $\pm$ 1.15
Sample	X203 (ug)	EE% Percentage	
Amount of X203 loaded	150	(93.18 $\pm$ 1.41) %	
Amount of X203 in supernatant	10.29 $\pm$ 2.12		

Table 1. 1 Single-layer HA X203 LbL NP Characterization (Zeta Size, Poly-Dispersity Index, Zeta Potential, and Encapsulation Efficiency)

$$\begin{aligned}
 \% \text{ EE} &= \frac{\text{Total amount of active agent} - \text{amount of active agent in the supernatant}}{\text{Total amount of active agent}} \times 100\% \\
 &= \frac{150\text{ug} - (10.29 \pm 2.12)\text{ug}}{150\text{ug}} \times 100\% \\
 &= \frac{(139.77 \pm 2.12)\text{ug}}{150\text{ug}} \times 100\% \\
 &= (93.18 \pm 1.41) \%
 \end{aligned}$$

Figure 4. 1 Calculation of HA X203 LbL NP Encapsulation Efficiency

From Table 1.1, it was evident that the particle was put together correctly. This can be seen from the zeta potential switching charges as additional layers were coated on. For instance, when PLA (positively charged) was coated onto HA (negatively charged), HA|PLA became highly positively charged ( $31.83 \pm 2.2\text{mV}$ ), indicating successful PLA coating. In the same way, HA|PLA|X203 was seen to be negatively charged ( $-13.37 \pm 1.21\text{mV}$ ) when x203 was coated onto positively charged HA|PLA. The X203 encapsulation efficiency (EE) was calculated to be  $139.77 \pm 2.12\mu\text{g}$  ( $93.18 \pm 1.41\%$ ).

HA is negatively charged due to the presence of hydroxide ions, a PLA layer is used to coat the negatively charged HA as PLA is positively charged due to the presence of guanidino group. To coat X203 electrostatically, it is important to disperse it in the ideal pH-adjusted medium to ensure maximum charge. To do so, its isoelectric point (pI) must be considered, which is essentially the pH at which the antibody has no net electrical charge. When the pH of the dispersant is below pI, the antibody will carry a net positive charge, with the reverse being true. As human antibodies have a pI range of around 8 – 9 [9], the X203 solution is prepared in NaCl (0.1M, pH 9.5), causing it to carry a maximum net negative charge.

The developed particle's (HA|PLA|X203|PLA) hydrodynamic diameter was about  $441.80 \pm 20.90\text{nm}$ , with a polydispersity index (PDI) of  $0.30 \pm 0.16$ . Though more optimization work could be done to better the size, the fabricated nanoparticle was already small enough to be effectively taken up into cells. Moreover, the particle's final surface charge was about  $27.00 \pm 1.15\text{mV}$ , giving them the ability to attach efficiently electrostatically onto cellular membranes (negatively charged) and improve cell uptake when dosed to cells.

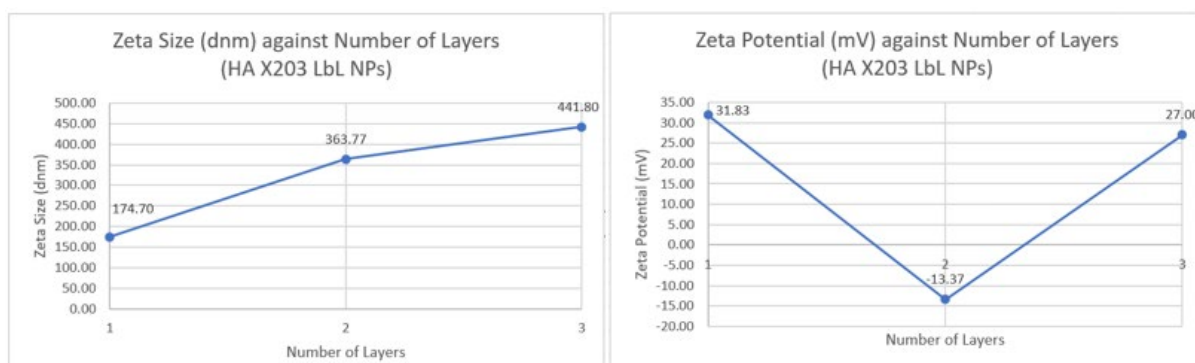


Figure 4. 2 Graph of Zeta Size (dnm) and Potential (mV) against number of layers

## 4.2 Functionality of the HA|PLA|X203|PLA LbL NPs

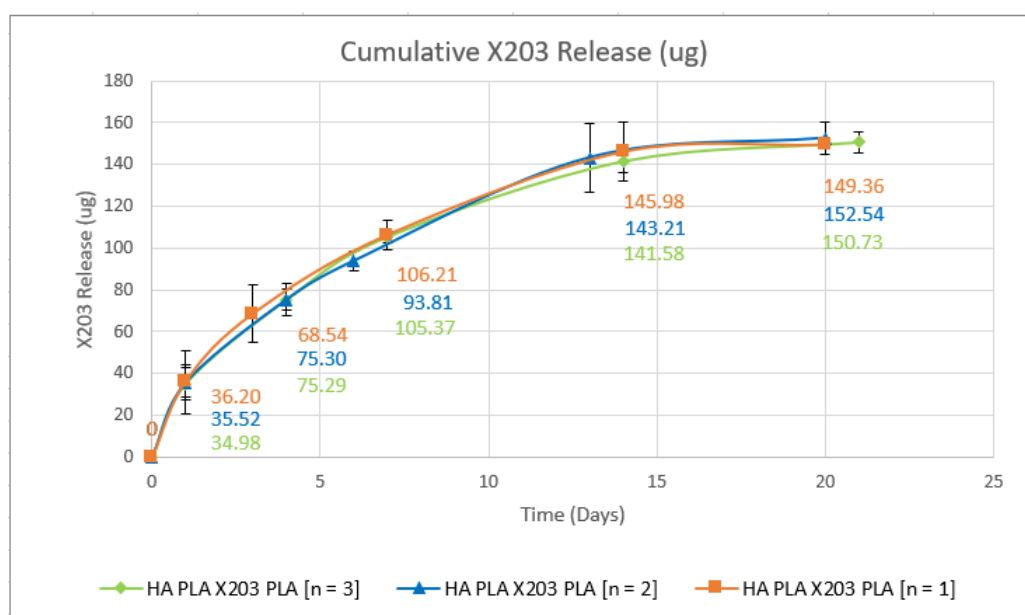


Figure 4. 3 Graph of Cumulative X203 Released (ug) over time (days).

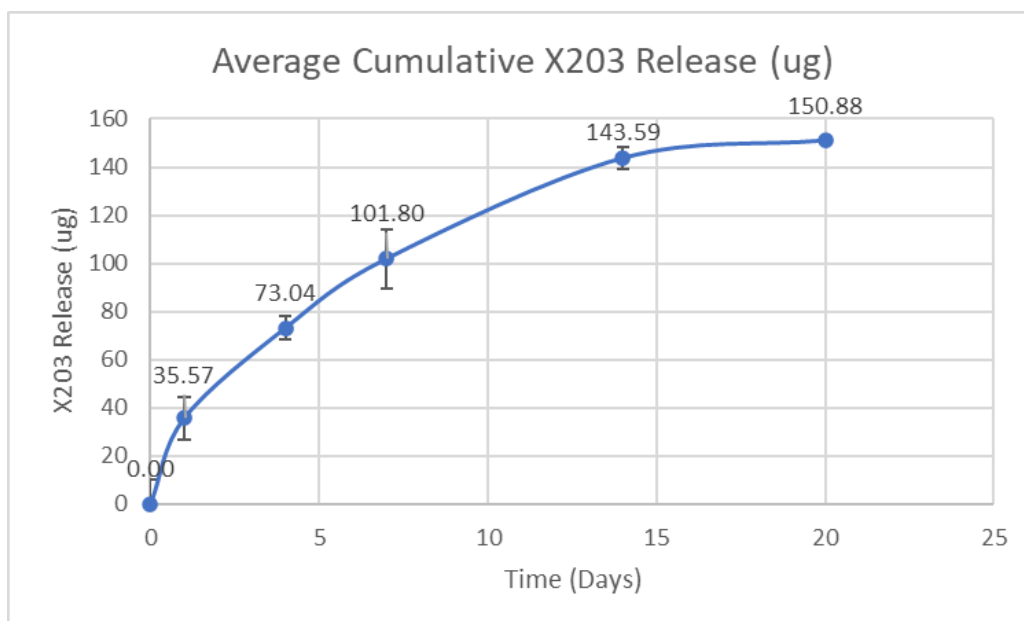


Figure 4. 4 Graph of Average Cumulative X203 Released (ug) over time (days).

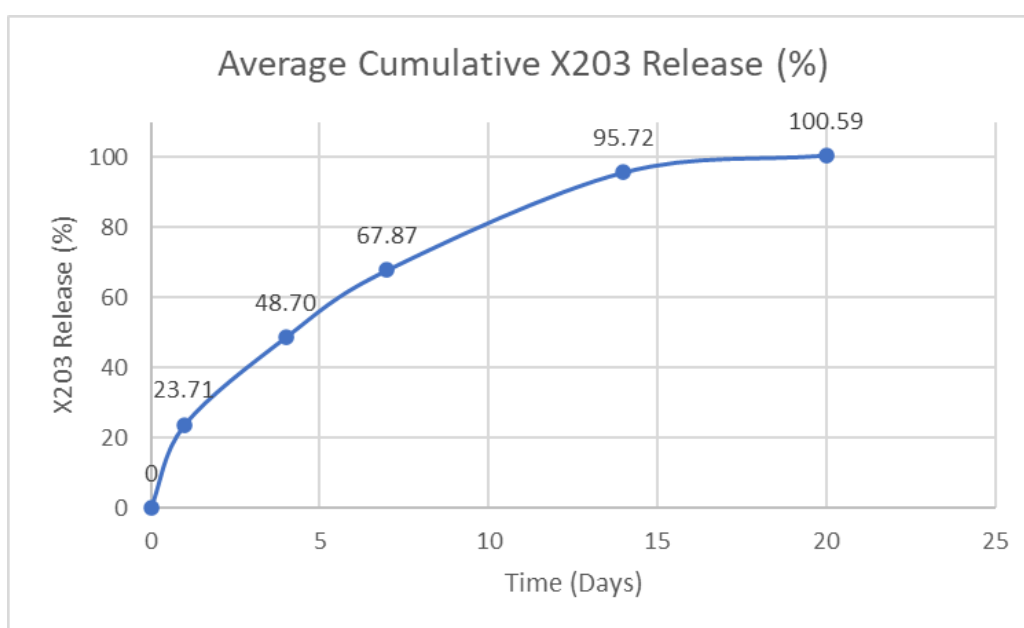


Figure 4. 5 Graph of Average Cumulative X203 Released (%) over time (days)

From the release profiles above, it was evident that the X203 loaded LbL NP (HA|PLA|X203|PLA) provide a prolonged sustained release of X203 over 14 – 20 days. An average cumulative X203 release of  $35.57 \pm 10.22\text{ug}$  (23.71%) at day 1,  $73.04 \pm 8.80\text{ug}$  (48.70%) at day 4,  $101.80 \pm 4.93\text{ug}$  (67.87%) at day 7,  $143.59 \pm 12.07\text{ug}$  (95.72%) at day 14, and  $150,88\text{ug} \pm 4.64\text{ug}$  (100.59%) at day 20 was observed, with the particles fully exhausting by day 14.

The prolonged sustained X203 release was made possible with the LbL system. The X203 layer was sandwiched between PLA layers. For the X203 release to happen, the outermost PLA layer must first defoliate. The PLA layers not only act as a platform for slow X203 release, they also help in protecting the X203 from degradation during fabrication and application. From the release profile, single-layered LbL NP can sustain release X203 up to 14 days with a single application.

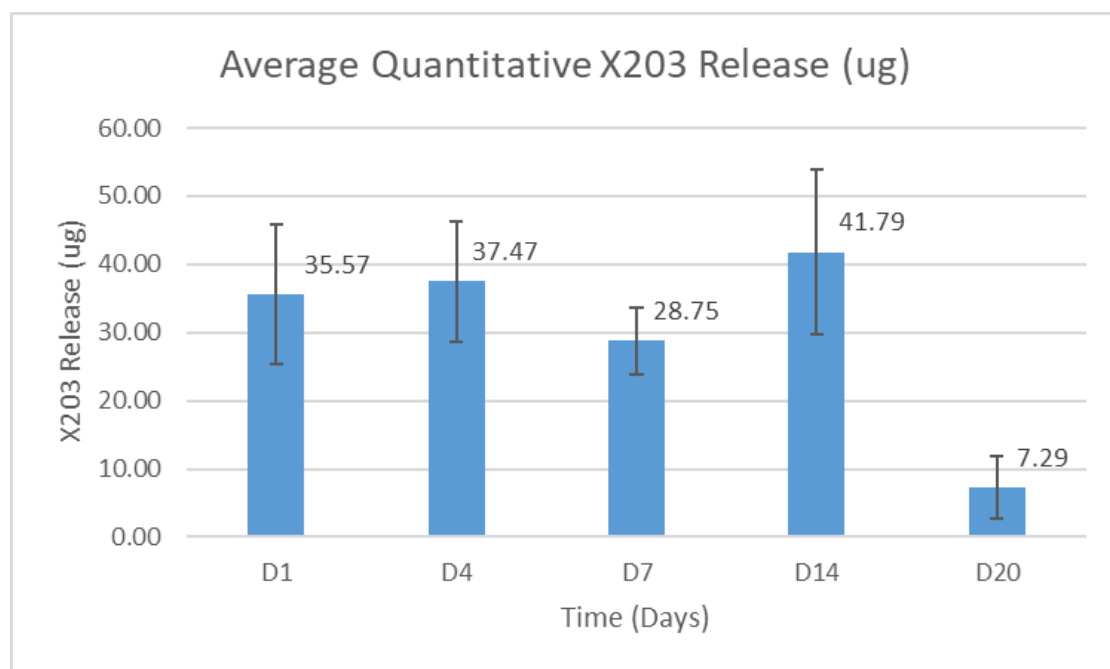


Figure 4. 6 Graph of Average Quantitative X203 Released (ug) over time (days).

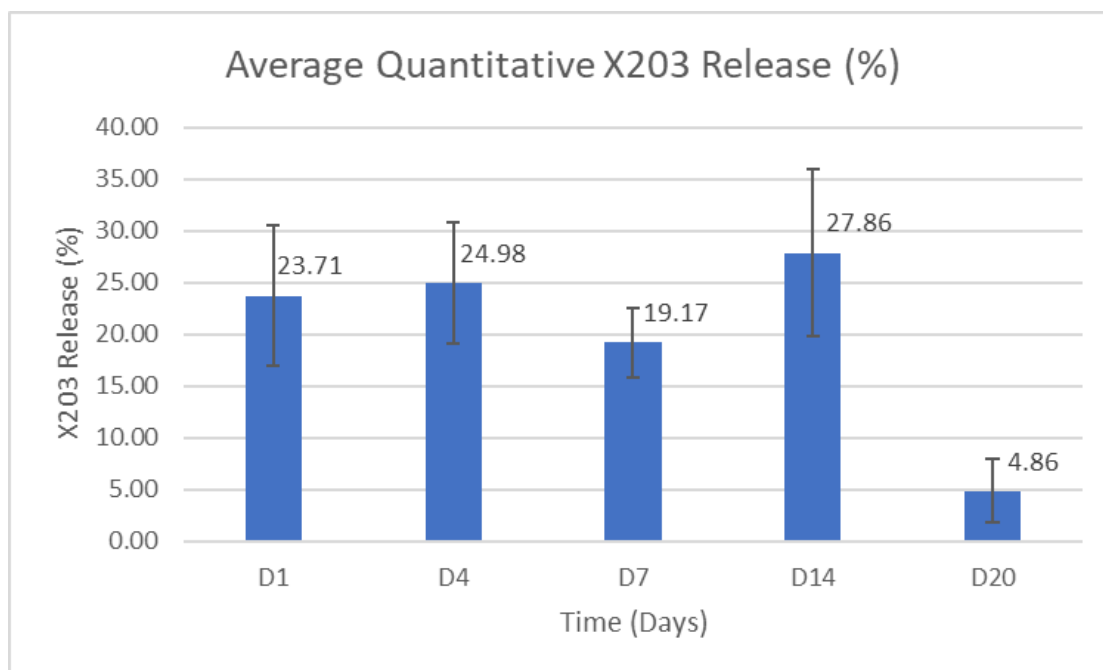


Figure 4. 7 Graph of Average Quantitative X203 Released (%) over time (days).

Based on Figure 4.5 it is evident that the single-layered HA|X203 LbL NP can sustain up to 14 days. However, we can see that at day 20 there are still residual X203 being released at an average of  $7.29 \pm 4.64$ . Hence, for a more accurate day at which X203 is fully exhausted, additional timepoints could be added between days 14 and 20. In addition, the quantitative release profile further proves that the release is controlled and sustained, due to its relatively consistent quantitative X203 release per timepoint when considering its lowest standard deviation of 23.71ug (15.81%) at day 1, 24.98ug (16.66%) at day 4, 19.17ug (12.79%) at day 7, and 27.86ug (18.57%) of X203 released on day 14. However, as there are gaps from days 7 to 14, there would undoubtedly be an increase in X203 release as the increment in timepoint is not the same as on days 1, 4, and 7. Hence, a consistent increment in timepoints is recommended.



### 4.3 Fabrication and characterization of HA|PLA|X203|PLA|X203|PLA LbL NPs

Particle configurations	Zeta size (dnm)	PDI	Zeta potential (mV)
HA PLA	204.40 ± 2.27	0.23 ± 0.01	34.03 ± 0.97
HA PLA X203	313.90 ± 2.85	0.19 ± 0.10	-14.03 ± 0.90
HA PLA X203 PLA	331.57 ± 0.06	0.31 ± 0.02	22.93 ± 3.18
HA PLA X203 PLA X203	492.07 ± 6.81	0.36 ± 0.04	-4.38 ± 0.50
HA PLA X203 PLA X203 PLA	439.17 ± 8.49	0.39 ± 0.15	10.45 ± 2.68

Table 2. Double Layer NPs Characterization with zeta size, PDI and zeta potential of all the layers

As shown in Table 2, the particle has alternating charges between the different layers which indicates successful coating of the double layer X203 NPs. As mentioned above, a highly positive charged HA|PLA (34.03 ± 0.97mV) shows a successful coating of the PLA layer on the HA. The HA|PLA|X203 layer being negatively charged (-14.03 ± 0.90mV) means that X203 was properly coated to the HA|PLA layer as X203 is negatively charged. The next PLA layer was also positively charged (22.93 ± 3.18mV). The HA|PLA|X203|PLA|X203 was also negatively charged (-4.38 ± 0.50) but the charge was lesser than the first X203 layer (-14.03 ± 0.90mV). Since the HA PLA X203 PLA particles were centrifuged before the second layer of X203 was coated, it might have resulted in lesser particles for the second X203 layer to coat on. The same could also be said for the final PLA layer as the HA|PLA|X203|PLA|X203 |PLA had a lesser positive charge (10.45 ± 2.68mV) as compared to HA|PLA|X203|PLA (22.93 ± 3.18mV). The final HA|PLA|X203|PLA|X203|PLA particle had a size of about 439.17 ± 8.49dnm with a PDI of 0.39 ± 0.15. Since the final particle size was under 500dmn, it is considered an acceptable size as the particle would be able to enter cells easily.

#### 4.4 Functionality of HA|PLA|X203|PLA|X203|PLA LbL NPs

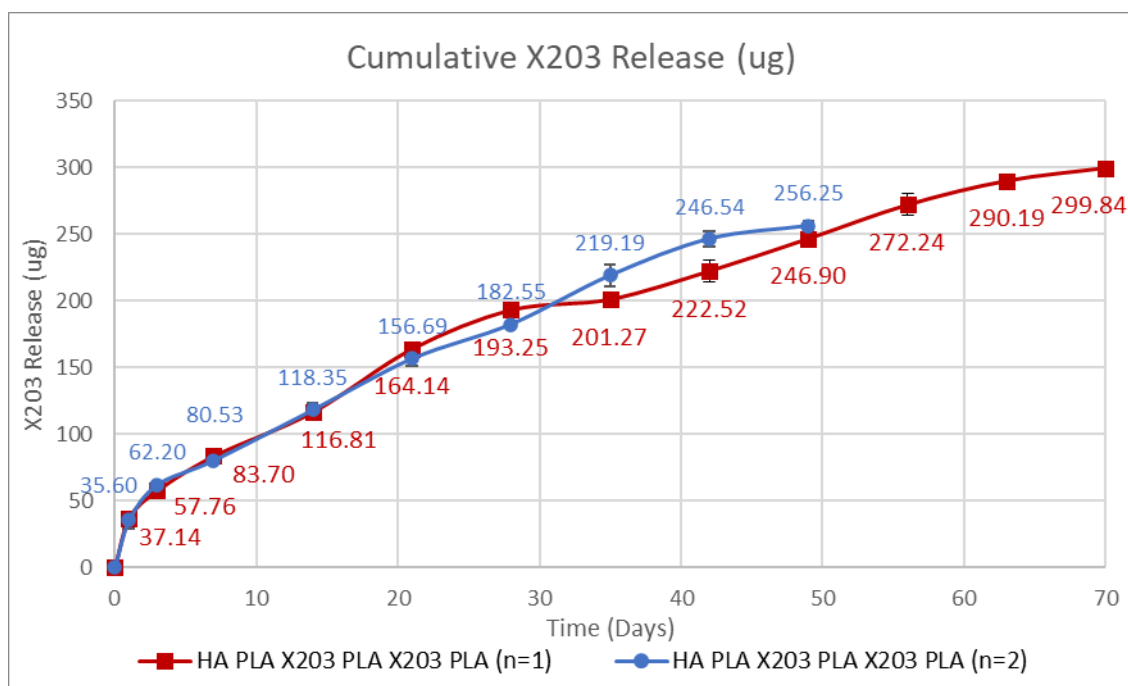


Figure 4.8 Graph of cumulative release of double layer X203 NPs(ug) over Time (Days)

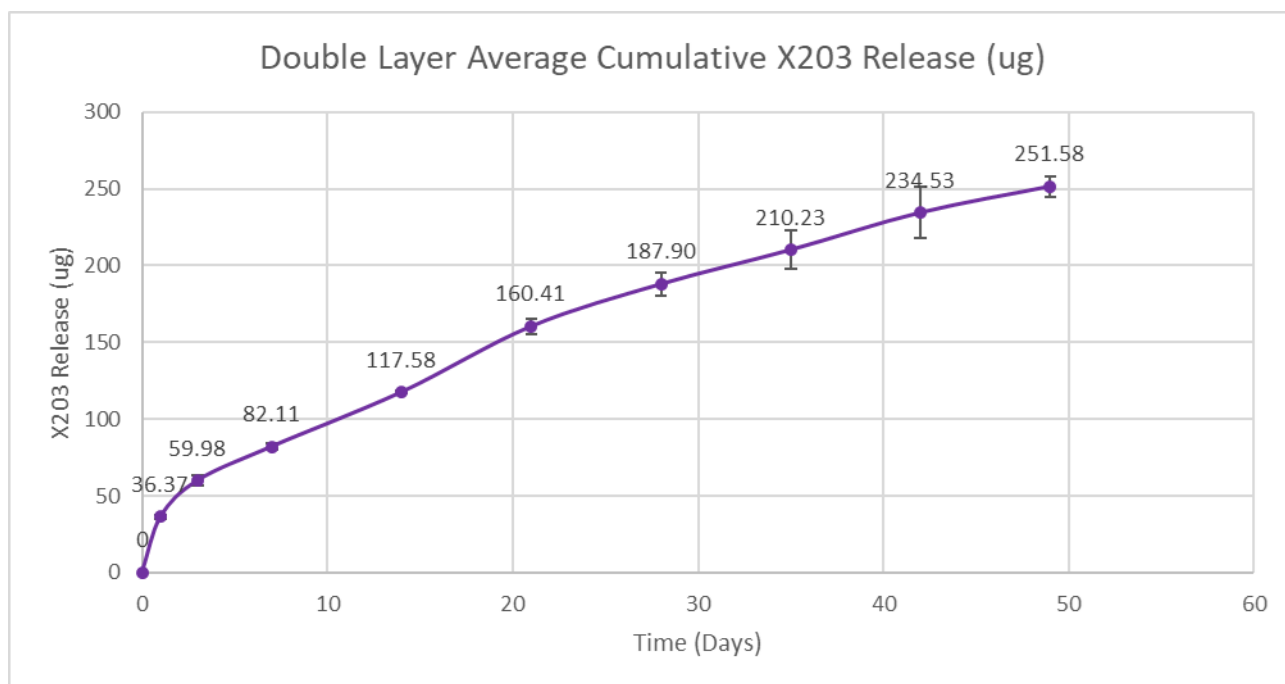
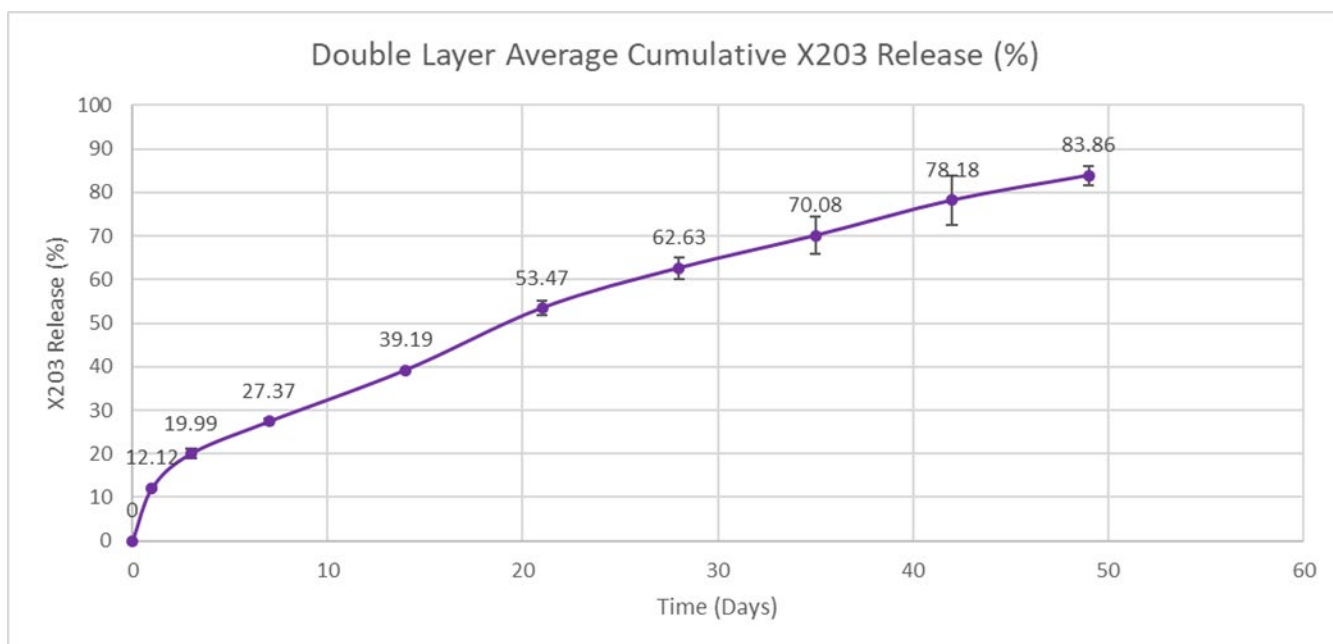


Figure 4.9 Graph of cumulative release of double layer X203 NPs (ug) over Time (Days)



*Figure 4.10 Graph of cumulative release of double layer X203 NPs (%) over Time (Days)*

From the graphs above, it is evident that the HA|PLA|X203|PLA|X203|PLA has a successful sustained release as it had been releasing for over 60 days. This is more than double the number of days compared to HA|PLA|X203|PLA. The total amount of X203 loaded for the double layer X203 NP was also 300ug, which is twice the amount when compared to the single layer X203. It can be seen in Figure 4.6 that the first batch of double layer X203 NPs has released the total loaded X203 and that it was plateauing as it reached the end. The average cumulative release of the double layer X203 was about 36.37ug (12.12%) on day 1, 59.98ug (19.99%) on day 3, 82.11ug (27.37%) on day 7, 117.58ug (39.19%) on day 14 and 160.41ug (53.47%) on day 21. However, after day 21 which was when most of the outermost layer of X203 was released, the rate of release slowed down. This can be concluded as even by day 49, which is more than double the number of days since day 21, the double layer X203 NP average cumulative release is 251.58ug (83.86%). This can also be seen in the next bar chart, which shows the average quantitative release from each time point.

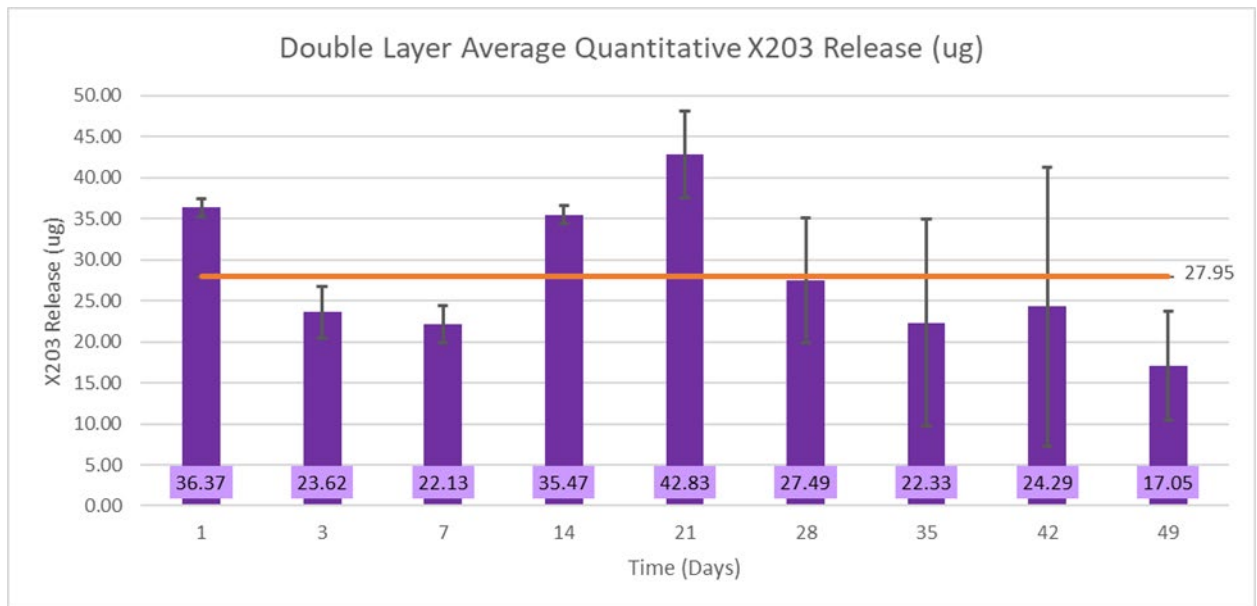


Figure 4. 11 Graph of average quantitative X203 release of double layer X203 NPs (ug) over Time (Days)

From Figure 4.11 above, the peak average quantitative release is day 21 with about 42.83ug. It is also seen that after day 21, that average X203 released slowed down. This is evident as the average release for each timepoint until day 21 is around 22 to 37 ug while the average release for each time point after day 21 is around 17 to 28ug. However, it is important to note that the first week had an additional timepoint taken at day 3. This could have affected the results of the subsequent weeks such as the peak of the average cumulative release which could have been on a different day from day 14 to day 21. Taking release studies on an additional day between the current weekly timepoints could have also helped us understand more about the release rate of the double layer X203 NP. Figure 4.9 also shows that the average quantitative release of all the timepoints is 27.95ug. However, most of the timepoints were below the average. This could be another sign that more timepoints are needed for a more accurate average quantitative release.

#### 4.5 Comparison of Single-layered vs Double-layered HA|X203 LbL NPs

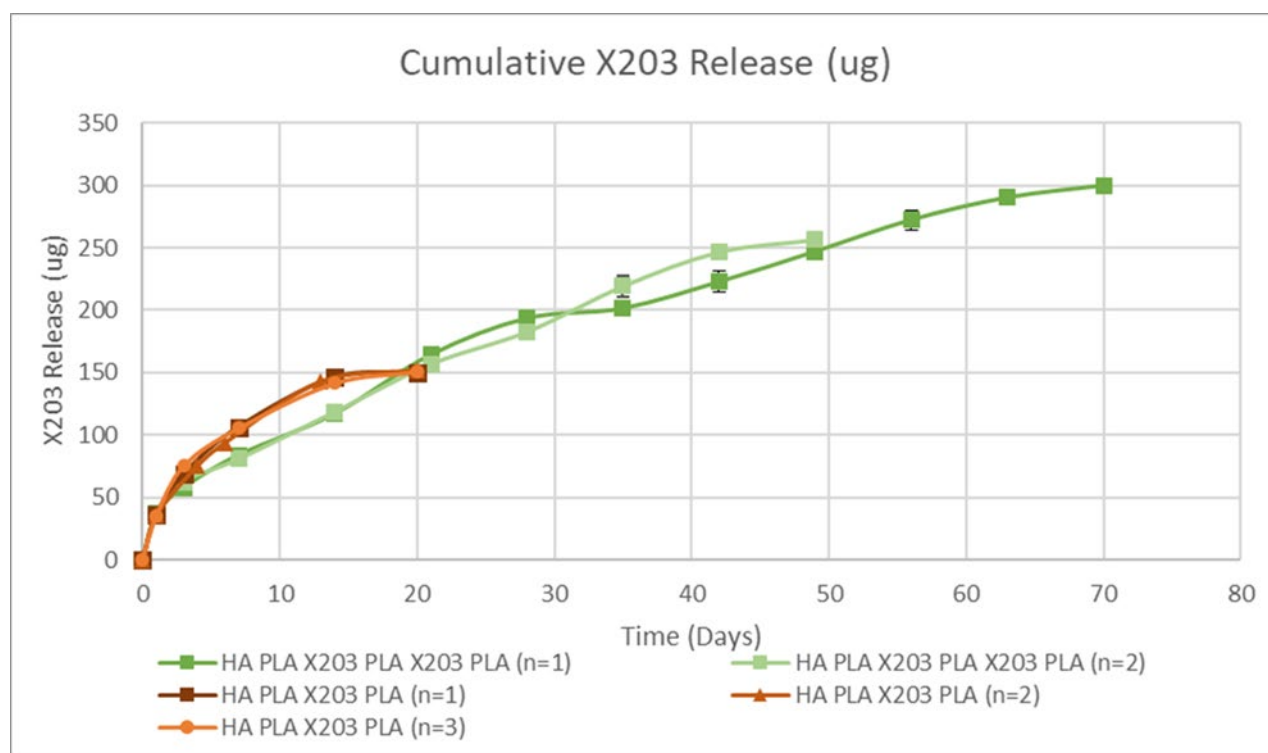


Figure 4. 12 Cumulative X203 Release graph of Single-layered X203 against Double-layered X203

As seen above, the single-layer X203 NP fully exhausted by day 14 while the double-layer X203 NP only released 116.81ug by then. This shows that the double-layer X203 has a slower release rate than the single-layer X203 NP. This might be due to the smaller charge of the outermost X203 layer of the double-layer X203 NP ( $-4.38 \pm 0.50\text{mV}$ ) as compared to the X203 layer of the single-layer X203 NP ( $-13.37 \pm 1.21\text{mV}$ ). The smaller charge of the double-layer X203 NP shows that lesser X203 was coated on the second X203 layer. Therefore, by day 14, there was more X203 released by the single X203 NP than the double-layer X203 NP.

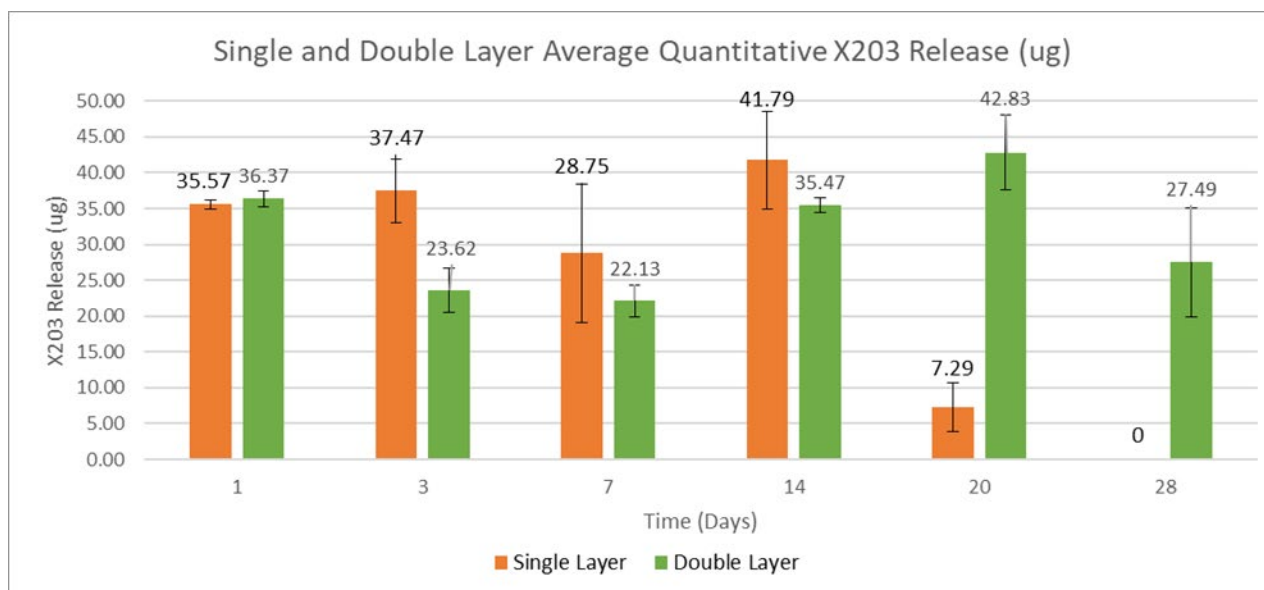


Figure 4. 13 Average Quantitative graph of Single-layered X203 against Double-layered X203

Figure 4.13 shows that the single-layer X203 NP peaked on day 14 at 41.79ug while the double-layer X203 peaked on day 20 at 42.83ug. It can also be seen that the trend for average quantitative release of the single-layer X203 NPs increased from 35.57ug to 37.47 ug, then decreased to 28.75ug, increased to 41.79ug then decreased to 7.29ug again. On the other hand, the trend of the double-layer X203 NPs decreased from 36.37ug to 23.62ug, then decreased to 22.13ug, then increased to 35.47ug, and then increased to 42.83ug. As mentioned above, the difference in trend could be because the charge of the outermost double-layer ( $-4.38 \pm 0.50\text{mV}$ ) is lesser than the charge of the X203 layer of the single-layer X203 NPs ( $13.37 \pm 1.21\text{mV}$ ). This causes the double-layer X203 NPs to have lesser X203 to be released than the single-layer X203 NPs. Additionally, while the double-layer X203 NPs were still releasing on day 28, the single-layer X203 NPs were already fully exhausted. This shows that the double-layer X203 NPs has a better sustained release than the single-layer X203 NPs.

## **5. CONCLUSION**

In conclusion, the project objectives have been successfully met by designing and developing nanocarriers (LbL NPs), using a negatively charged HA as the structural core and positively charged PLA as polymer layers to incorporate anti-IL-11 antibody (X203) with the expected characterization specifications to provide a prolonged sustained release effect. Nanocarriers developed were of hydrodynamic size less than 500nm, with the X203 successfully encapsulated between PLA layers through electrostatic interactions. All in all, the nanocarriers developed were successful as they were able to provide a prolonged sustained release effect of X203 of up to 14 days for single-layered X203 nanocarriers and up to 70 days for double-layered X203 nanocarriers through conducted release studies.

However, these nanocarrier systems can still be improved upon, such as by exploring other molecular weights of PLA. In addition, as size of particle and encapsulation is highly dependent on the parameters of the microfluidic device (IGNITE machine) (flow rate, flow ratio, and concentration), further optimization of microfluidic device setting is also recommended.

**Word count (excluding cover page, headings, sections, captions, and references): 3167**

## **Acknowledgments**

The author wishes to thank the collaboration partner National University of Singapore, Institute of Health and Technology for their generosity and kind assistance: Prof. Subbu Venkatraman, Principal Investigator; Dr. Yang Fei Tan, Research Fellow; Mr. Muhammad Aminuddin Bin Anuar, Research Engineer. The author would also like to extend their gratitude towards MP supervisor, Dr. Raja Rangaswamy, Senior Lecturer, for his guidance and support.

## References

- [1] Anti-IL-11 antibody. *Biosynth Laboratories*. (2023, July 3). [Online]. Available: <https://crbdiscovery.com/discovery-antibodies/anti-il-11-antibody/>
- [2] IL-11: Products. *Rndsystems* (n.d.). [Online]. Available: [https://www.rndsystems.com/target/il-11?category=Primary+Antibodies&gclid=CjwKCAjwxr2iBhBJEiwAdXECw\\_6l99EVfdociTwJ2i2sqKwH7u0xjzqdDDo9lUMPe1UepHUI55gUQBoCbC0QAvD\\_BwE&gclsrc=aw.ds](https://www.rndsystems.com/target/il-11?category=Primary+Antibodies&gclid=CjwKCAjwxr2iBhBJEiwAdXECw_6l99EVfdociTwJ2i2sqKwH7u0xjzqdDDo9lUMPe1UepHUI55gUQBoCbC0QAvD_BwE&gclsrc=aw.ds)
- [3] Ng, B., Cook, S.A. & Schafer, S. Interleukin-11 signaling underlies fibrosis, parenchymal dysfunction, and chronic inflammation of the airway. *Exp Mol Med* **52**, 1871–1878 (2020). [Online]. Available: <https://doi.org/10.1038/s12276-020-00531-5>
- [4] Din, F. ud, Aman, W., Ullah, I., Qureshi, O. S., Mustapha, O., Shafique, S., & Zeb, A. (2017, October 5). *Effective use of nanocarriers as drug delivery systems for the Treatme: IJN*. International Journal of Nanomedicine. [Online]. Available: <https://www.dovepress.com/effective-use-of-nanocarriers-as-drug-delivery-systems-for-the-treatme-peer-reviewed-fulltext-article-IJN>
- [5] Cao, Y., Tan, Y.F., Wong, Y.S. et al. Designing siRNA/chitosan-methacrylate complex nanolipogel for prolonged gene silencing effects. *Sci Rep* **12**, 3527 (2022). [Online]. Available: <https://doi.org/10.1038/s41598-022-07554-0>
- [6] N. Boehnke, S. Correa, L. Hao, W. Wang, J. P. Straehla, S. N. Bhatia, P. T. Hammond, *Angew. Theranostic Layer-by-Layer Nanoparticles for Simultaneous Tumor Detection and Gene Silencing Chem. Int. Ed.* 2020, **59**, 2776. [Online]. Available: [https://onlinelibrary.wiley.com/doi/10.1002/anie.201911762#:~:text=Layer%2Dby%2Dlayer%20nanoparticles%20\(polyelectrolytes%20onto%20charged%20nanoparticle%20cores](https://onlinelibrary.wiley.com/doi/10.1002/anie.201911762#:~:text=Layer%2Dby%2Dlayer%20nanoparticles%20(polyelectrolytes%20onto%20charged%20nanoparticle%20cores)
- [7] Esfahani, D. R., Tangen, K. M., Sadeh, M., Seksenyan, A., Neisewander, B. L., Mehta, A. I., & Linninger, A. A. *Computer Aided Chemical Engineering*. Computer Aided Chemical Engineering | Quantitative Systems Pharmacology - Models and Model-Based Systems with Applications |, “Chapter 9 - Systems engineers’ role in biomedical research. Convection-enhanced drug delivery,” vol. 42, 2018, pp. 271-302. [Online]. Available: <https://www.sciencedirect.com/science/article/abs/pii/B978044463964600009X>
- [8] S. S. I. A. E. T. Munir MU, “Synthesis, Characterization, Functionalization and Bio-Applications of Hydroxyapatite Nanomaterials: An Overview,” vol. 2022, no. 17, pp. 1903-1925, 2022. [Online]. Available: <https://www.dovepress.com/synthesis-characterization-functionalization-and-bio-applications-of-h-peer-reviewed-fulltext-article-IJN>
- [9] Morga, M., Batys, P., Kosior, D., Bonarek, P., & Adamczyk, Z. (2022). Poly-L-Arginine Molecule Properties in Simple Electrolytes: Molecular Dynamic Modeling and Experiments. *International journal of environmental research and public health*, **19**(6), 3588. [Online]. Available: <https://doi.org/10.3390/ijerph19063588>



[10] Schneider, Z. (2017, June 28). *Importance of isoelectric point ( $p_i$ ) of antibodies*. The Antibody Society. [Online]. Available: <https://www.antibodysociety.org/new-articles/importance-isoelectric-point-pi-antibodies/>